

SUPPLEMENTARY INFORMATION

Supplemental methods

Generation of KCNE3 null mice- Primers were designed to amplify two contiguous DNA fragments of 5.08 kb (long arm) and 2.9 kb (short arm) containing the exons 1 to 3 and 4 respectively, from 129/SvJ genomic DNA. PCR products were subcloned into a modified pBluescript (Stratagene) containing a neomycin resistance cassette for positive selection, and thymidine kinase (tk) and diphtheria toxin (dta) genes to select against random insertions. LoxP sites were added flanking the fourth exon and the neomycin resistance cassette for further gene inactivation by excision using the cre recombinase. Relative positions of these different elements are shown in Figure S1A. This construct was verified by sequencing the KCNE3 coding sequence, 5' and 3' ends of long and short arms, as well as the loxP sites and the regions flanking the neo cassette. After linearization, the targeting vector was transfected by electroporation into R1 embryonic stem cells. Probes used in Southern blot analysis were located outside of the region encompassed by the vector (Fig. 1A). They were generated by PCR from genomic *kcne3* sequence (a 5' probe of 515 bp generated with primers CACTCTGGGTCTTTTGAATCC and CCACATCCAAATTGTTTCTGA, and a 3' probe of 740 bp with CAAAGAAGGAGGAAAAGGAA and ATAAAGGGCTGGCTCTGAAA). In correctly targeted clones, these probes detect bands of 6 and 8 kb, in *Bgl*I digested genomic DNA, respectively.

Correctly targeted cells were injected into C57BL/6J blastocysts that were implanted into foster mothers. Chimeric males were bred with C57BL/6J females and subsequently crossed with cre-deleter mice (1) (in C57BL/6J background). The neomycin selection cassette and the coding region (exon 4) were removed and the new sized band of 9.5 kb was confirmed by Southern blot analysis (Fig. 1B).

Intestinal fluid secretion measurement- Wild-type or *kcne3*^{-/-} mice (body weight 20-22 g) were deprived of food 24 h prior to experiments. Cholera-toxin stimulated intestinal fluid secretion was determined essentially as described (2,3). Briefly, animals were anaesthetized by exposure to isoflurane using the Univentor 400 anesthesia unit (Univentor, Zejtun, Malta) at air flow rate 400 - 500 ml/min, 4% isoflurane. Mice were kept anaesthetized by exposure to 2% isoflurane using a mask and a constant flow rate (150 - 250 ml/min). Body temperature was maintained by placing the mouse on a heating pad (maintained at 38°C). A small abdominal incision exposed the small intestine. Ileal loops (~20 mm) proximal to the caecum were exteriorized and isolated (2-3 loops per mouse). The closed loops were injected with 100 µl of PBS alone or PBS containing cholera toxin (0.5 µg per loop) (Gentaur, Kampenhout, Belgium). The wound was sutured, and mice were kept under isoflurane anaesthesia for 5h. They were then sacrificed, intestinal loops removed, weighed with and without fluid contents, and their length measured.

Patch clamp of mouse colonic crypts- Mouse colonic crypts were prepared as described for rat (4). Mice were killed by cervical dislocation. A 3 cm piece of mouse distal colon was everted and rinsed with ice-cold 'colon' solution containing (in mM) 127 NaCl, 5 KCl, 5 Na-pyruvate, 5 D(+)-glucose, 10 HEPES, 1 MgCl₂, 1.3 CaCl₂, pH 7.4. Both ends were tied and the resulting sac was filled with a Ca⁺⁺-free solution containing (in mM) 127 NaCl, 5 KCl, 5 Na-pyruvate, 5 D(+)-glucose, 10 HEPES, 1 MgCl₂, 5 EDTA, pH 7.4 and then incubated in "Ca⁺⁺-free" solution for 11 min at 37°C. Isolated crypts were obtained by shaking these sacs in 'colon' solution. Crypts were transferred into a bath chamber (held at 37°C) mounted on the stage of an inverted microscope and held by a suction pipette. Individual crypt base and crypt middle cells were patch-clamped (mean pipette resistance of 6-10 MΩ. Internal solution (in mM): 95 K-gluconate, 30 KCl, 1.2 NaH₂PO₄, 4.8 Na₂HPO₄, 0.7 CaCl₂, 2.4 MgCl₂, 1 EGTA, 5 D(+)-glucose, 3 ATP). The bath solution contained (in mM): 145 NaCl, 1.6

K₂HPO₄, 0.4 KH₂PO₄, 1.3 CaCl₂, 1 MgCl₂, 5 D(+)-glucose, 5 HEPES, pH 7.4. Recordings were obtained in whole-cell mode using an EPC7-like amplifier (U. Fröbe, Freiburg, Germany).

Supplemental Results

KCNQ1/KCNE3 currents of colonic crypt cells. Currents from mid-basal colonic crypt cells were measured in the whole-cell configuration of the patch-clamp technique (Fig. S5). Unfortunately, attempts to experimentally eliminate chloride currents by using chloride-free solutions failed because cells appeared unhealthy and no stable patches could be obtained. Experiments were therefore performed in normal Ringer's. Under these conditions, forskolin is expected to increase CFTR-mediated Cl⁻ currents and K⁺ currents through KCNQ1/KCNE3 channels (5). Both channel types are activated by cAMP.

Both WT and KO colonic crypt cells displayed whole-cell currents that depended nearly linearly on voltage (Suppl. Fig. S5A). Consistent with a reduced K⁺ conductance, currents from *kcne3*^{-/-} cells were about 30% smaller than those from WT cells and reversed at a slightly more positive voltage. In the presence of forskolin, WT and KO crypt cells depolarized (Suppl. Fig. S5B-D), compatible with a prominent Cl⁻ current component carried by CFTR in cells of both genotypes. Under our ionic conditions, the Cl⁻ reversal potential is calculated to -37 mV. Again, currents of KO cells showed a more positive reversal potential that is compatible with a partial loss of a K⁺ conductance. Surprisingly, but similar to results obtained by others (6), the whole cell conductance was not increased by forskolin, even though cAMP should increase currents through both CFTR and KCNQ1/KCNE3. This result can only be explained by a concomitant downregulation of other conductances, e.g. KCNN4 or ENaC channels. We next evaluated the C293B-sensitive current after stimulation by forskolin (Suppl. Fig. S5B,D-F). This current component, which accounts for about 20% of whole cell current under our experimental conditions, was nearly totally abolished in *kcne3*^{-/-} crypt cells (Suppl. Fig. S5E,F).

Supplemental figure legends:

Fig. S1. Histology of several hematoxylin/eosin (H/E) stained tissues from 1 year-old WT and *kcne3*^{-/-} mice. *A & B*, stomach. *C & D*, small intestine. *E & F*, colon. *G & H*, trachea. *I-L* transversal (*I,J*) and longitudinal (*K,L*) sections of hindlimb skeletal muscle. *M & N* hippocampus. *O & P* cerebellum. Scale bars denote same lengths for KO and WT. No obvious morphological differences were observed between tissues from the two genotypes.

Fig. S2. Specificity of the anti-KCNE3 antibody. *A.* Western blot analysis of cells transfected with a construct encoding an N-terminally HA-tagged version of KCNE3 (lane T) and native COS-7 cells (lane NT). The anti-HA antibody detected a band pattern (between 20 and 30 kDa, arrowhead) in KCNE3-transfected COS cells, which was absent from non-transfected cells. *B.* A faint but similar band pattern (arrowhead) was detected in a membrane fraction of WT colon; it was absent from the KO. The asterisk (*) indicates a KCNE3-immunoreactive, high-molecular weight band, which might represent SDS-resistant KCNE3 aggregates. *C.* After deglycosylation of cell membrane lysates by PNGaseF the KCNE3 antibody recognized a single band (~14 kDa, arrowhead) in WT colon membranes that was absent from the KO. COS-7 cells overexpressing HA-KCNE3 were used as positive control (lane T). The presence of several bands in the latter lane might be owed to incomplete deglycosylation caused by the N-terminal HA tag.

Fig. S3. Western blot on membrane preparation from gastrointestinal tissues shows no difference in KCNQ1 protein amount between WT and *kcne3*^{-/-} mice. Top, colonic membranes from 3 different WT/KO mouse pairs. Below, membranes from colon, jejunum,

ileum and stomach from a different mouse pair. Equal amounts of proteins (~50 µg) were loaded and α-actin served as loading control.

Fig. S4. No difference in cholera toxin-mediated small intestinal fluid secretion between WT and *Kcne3*^{-/-} mice. *A & B.* Representative ileal loops 5 h after luminal injection of PBS alone (left ligated loop) and PBS + cholera toxin (CTx 0.5 µg per loop) (right ligated loop) from WT (A) and *kcne3*^{-/-} mice (B). *C.* Average loop mass/length from WT and KO mice 5 h after injections. There are no statistically significant differences between the two genotypes. Mean ± SEM, n=3 each.

Fig. S5. Whole-cell currents from WT and *kcne3*^{-/-} colonic crypt cells. *A & C.* Current/voltage relationship of WT (♦) and KO (□) colonic crypt cells under control conditions (A) and after addition of 10 µM forskolin (C). Number of cells: (A), 10 WT, 9 KO; (C) 10 WT, 7 KO. *E.* C293B-inhibitable current component of WT (♦) and KO (□) colonic crypt cells obtained by subtracting currents recorded in the presence of FSK from those in the presence of both FSK and C293B (10 WT and 7 KO) cells). *B & D.* Representative current traces recorded from WT (B) and KO (D) colonic crypts during superfusion with control- (left), FSK- (middle) and FSK + C293B-containing solutions (right). From a holding potential of -95 mV, the voltage was clamped for 2 s to values between -95 and +25 mV (protocol shown in inset (D)). *F.* Representative traces of C293B-sensitive current component recorded from WT and KO crypt cells. Inset, voltage-clamp protocol. Cells recorded were from the lower third of isolated crypts. Mean values ± SEM are shown. *, p<0.05. **, p<0.005

Table 1. Urine, feces, and serum parameters from WT and *kcne3*^{-/-} mice. Electrolyte and protein levels in urine were normalized to creatinine. Na⁺ and K⁺ concentrations in feces were normalized to the dry weight of feces as described in Experimental Procedures. There is no statistically significant difference between WT and KO mice in any of the measured parameters. Mean ± SEM. n, number of animals.

Supplemental References

1. Schwenk, F., Baron, U., and Rajewsky, K. (1995) *Nucleic Acids Res* **23**, 5080-5081
2. Ma, T., Thiagarajah, J. R., Yang, H., Sonawane, N. D., Folli, C., Galletta, L. J., and Verkman, A. S. (2002) *J Clin Invest* **110**, 1651-1658
3. Rufo, P. A., Merlin, D., Riegler, M., Ferguson-Maltzman, M. H., Dickinson, B. L., Brugnara, C., Alper, S. L., and Lencer, W. I. (1997) *J Clin Invest* **100**, 3111-3120
4. Ecke, D., Bleich, M., Schwartz, B., Fraser, G., and Greger, R. (1996) *Pflügers Arch* **431**, 419-426
5. Schroeder, B. C., Waldegger, S., Fehr, S., Bleich, M., Warth, R., Greger, R., and Jentsch, T. J. (2000) *Nature* **403**, 196-199
6. Diener, M., Hug, F., Strabel, D., and Scharrer, E. (1996) *Br J Pharmacol* **118**, 1477-1487

Fig. S1

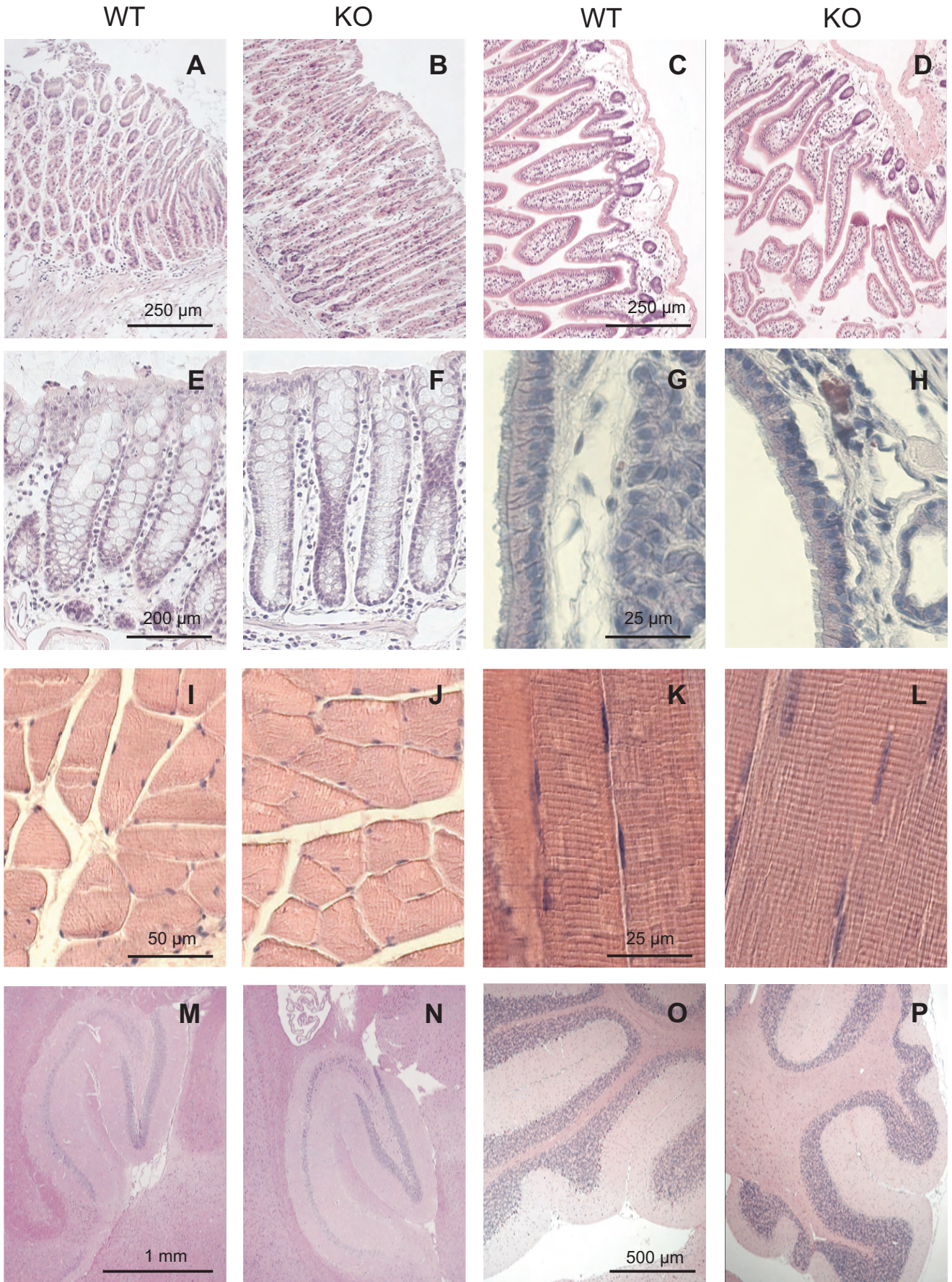
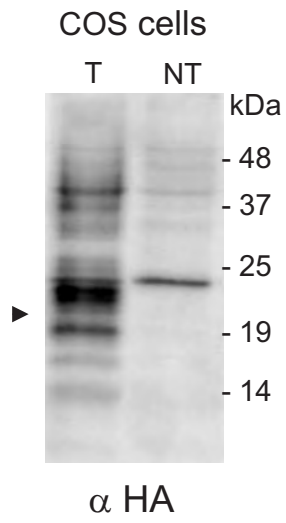
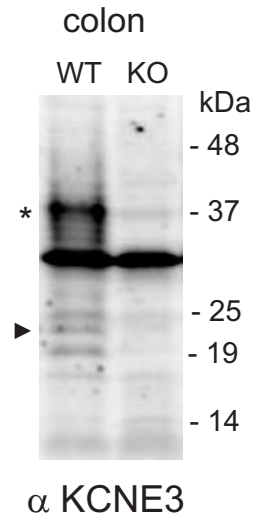


Figure S2

A



B



C

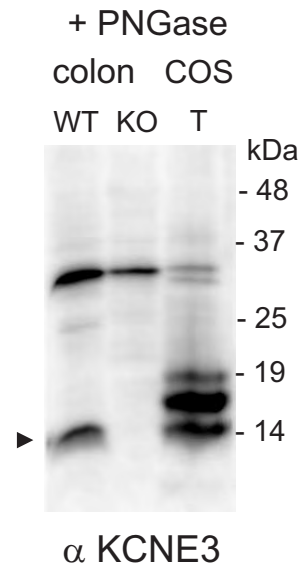


Figure S3

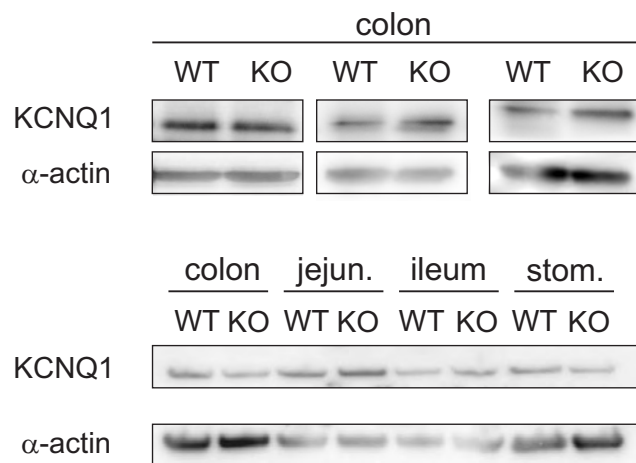


Figure S4

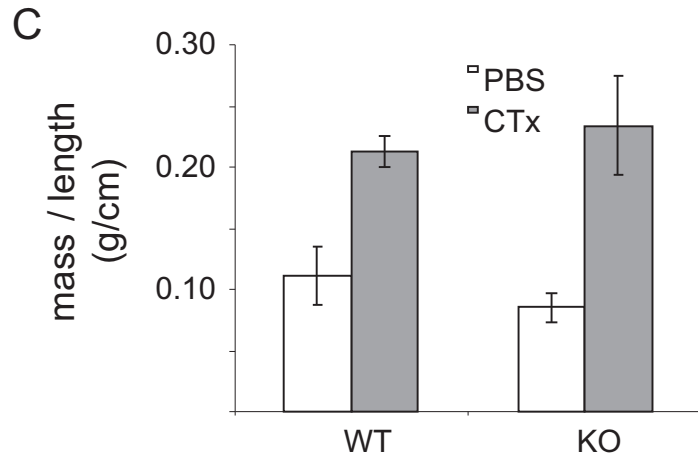
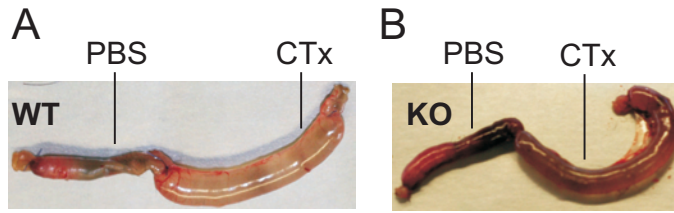


Figure S5

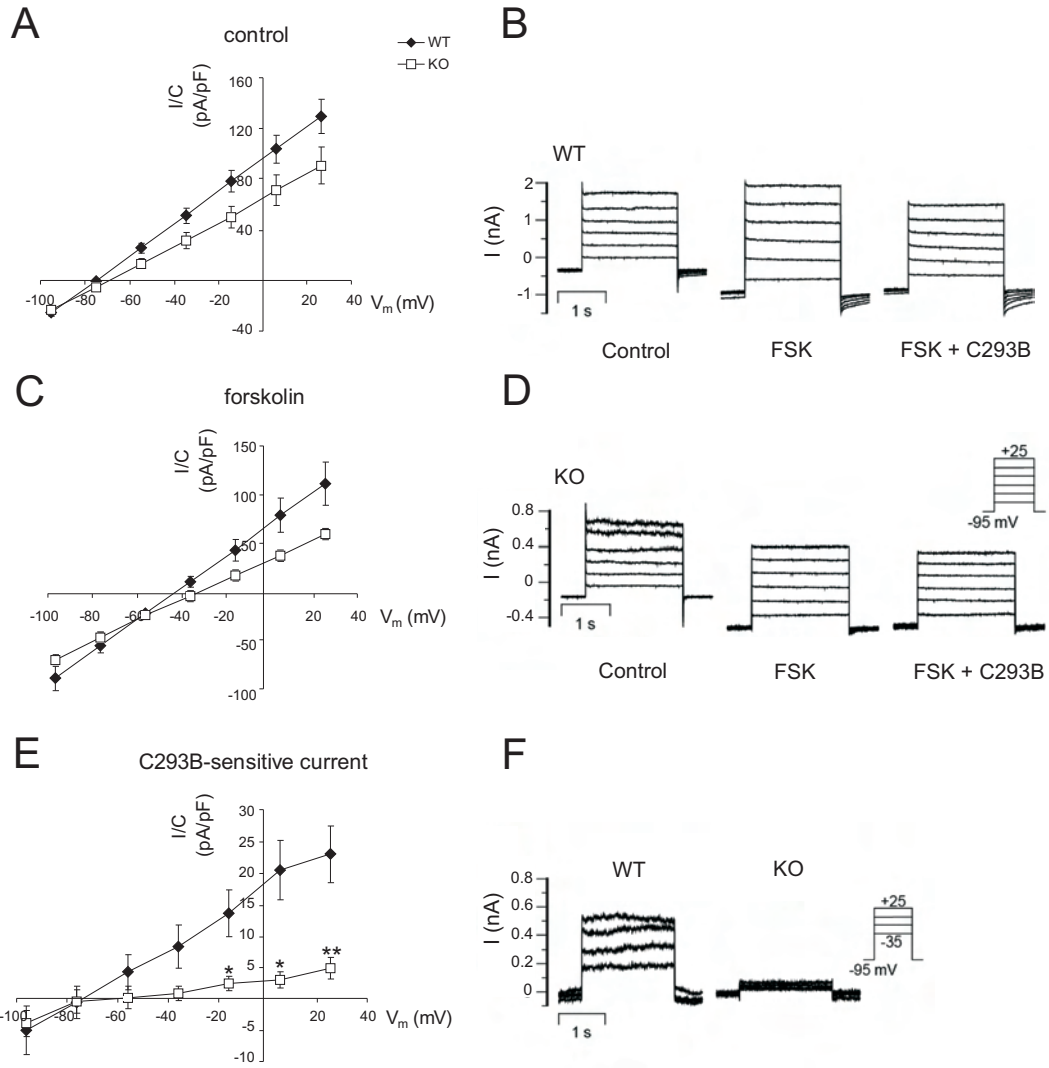


Table 1

		<i>kcne3</i> ^{+/+}	<i>kcne3</i> ^{-/-}
urine (n=6)	creatinine (mM)	2.6 ± 0.5	3.1 ± 0.31
	K/creatinine (mmol/mmol)	112.2 ± 5.7	104.3 ± 6.1
	Na/creatinine (mmol/mmol)	39 ± 1.7	37.6 ± 2.5
	Cl/creatinine (mmol/mmol)	75.6 ± 3.8	68.8 ± 2.9
	Ca/creatinine (mmol/mmol)	0.8 ± 0.1	1.2 ± 0.6
	Mg/creatinine (mmol/mmol)	8.6 ± 0.6	7.7 ± 1.2
	Pi/creatinine (mmol/mmol)	14.8 ± 2.1	14 ± 1.7
	protein/creatinine (mg/mg)	29.6 ± 2.7	28.5 ± 2.2
feces (n=4)	Na μmol/gr dry weight	40.7 ± 10.2	28 ± 8.5
	K μmol/gr dry weight	137.6 ± 32.2	81.9 ± 25.7
serum (n=8)	K (mM)	7.2 ± 0.8	6.3 ± 1
	Na (mM)	131.2 ± 5.6	126.7 ± 2.3
	Cl (mM)	96.8 ± 3.8	93.4 ± 2.7
	Ca (mM)	1.9 ± 0.1	2.1 ± 0.1
	Mg (mM)	1.3 ± 0.1	1.3 ± 0.1
	protein (g/dL)	3.8 ± 0.2	3.9 ± 0.1
	phosphorus (mM)	3.6 ± 0.3	3.1 ± 0.1
	glucose (mM)	16.4 ± 1.7	14.9 ± 1.5
	ALP IU/L	71.3 ± 0.8	62.4 ± 3.5